

Thermal Cycling Behaviour of Dense Monolithic Alumina

Luís Guerra Rosa^{1*}, José Rodríguez², José C. G. Pereira³ and Jorge C. Fernandes¹

¹IDMEC, IST, Universidade de Lisboa, Av. Rovisco Pais, Lisboa, Portugal

²Plataforma Solar de Almería, CIEMAT, Tabernas (Almería), Spain

³DEQ, IST, Universidade de Lisboa, Av. Rovisco Pais, Lisboa, Portugal

Keywords: Alumina, Thermal Cycling, Concentrated Solar Radiation.

Abstract: The behaviour of circular discs, with 25 mm diameter and 2 mm thickness, made of commercial high-purity dense monolithic Alumina (RAPAL® 100) is evaluated under three different sequences of 100 heating-cooling cycles, all of them with a maximum temperature of 1200°C. None of the different sequences of 100 cycles (even the most severe one with 100 cycles applied in 77 minutes, with maximum temperature of 1200°C and minimum temperature of 400°C) has caused noticeable alterations in the studied properties (density; Young's modulus of elasticity; Coulomb's modulus of elasticity; flexural strength) measured before and after the heat treatment.

1 INTRODUCTION

The increasing demand of ceramic materials for structural applications – namely in components for wear resistance and high temperature use – stresses the need for a deeper knowledge and correct characterization of their mechanical behaviour. In their nature, ceramics are brittle and critically dependent of the presence of flaws (porosity, internal and surface cracks, etc.) which are responsible, not only for a significant decrease in strength, but also for a high scatter in data. In brittle materials, strength may be seen as a consequence of two factors: (1) fracture toughness (K_{Ic} , an intrinsic value of the material), and (2) the distribution (in size and orientation) of the population of flaws that are present in the specimens or test-pieces. A flaw, geometrical discontinuity or other heterogeneity, that causes an effect of stress/strain concentration and it is responsible for the rupture is named “critical flaw”.

For many applications of technical or advanced ceramics, it is important to evaluate their behaviour when they are exposed to high-temperature cycles and rapid cooling at the surface. If the temperature to which a test-piece is exposed varies rapidly i.e. if it is subjected to “thermal shock”, a difference in temperature between the surface and the bulk of the test-piece will be generated, and this will create mechanical stresses of high magnitude. These high-magnitude stresses can cause the growth of pre-

existent flaws, thus leading to the degradation of some of the mechanical properties. According to (Evans et al., 1975) the stress σ_T caused by a thermal shock ΔT is given by:

$$\sigma_T = \frac{E \alpha \Delta T}{1 - \nu} f(\beta) \quad (1)$$

where E is Young's modulus, α is the linear thermal expansion coefficient, ν is Poisson's ratio, and $f(\beta)$ is a function that introduces the influence of the geometry of the test-piece that is subjected to thermal shock. β is known as the Biot modulus, defined as:

$$\beta = \frac{b h}{k} \quad (2)$$

where b is a specimen dimension, h is the heat transfer coefficient and k is the thermal conductivity of the specimen or test-piece. Consequently, we may notice that the determination of thermal stresses caused by thermal shock is not easy because the values of the heat transfer coefficient h and the function $f(\beta)$ must be known with significant precision. On the other side, as suggested by (Hirata, 2015), the linear thermal expansion coefficient α of a material has not a constant value because it depends on temperature and microstructure of the material.

In comparative terms, alumina (Al_2O_3) is to technical ceramics what mild steel is to metals – it is

relatively cheap, easy to process, and it has a wide range of industrial applications. Pure alumina has a melting point of 2072°C, therefore alumina components are used at operating temperatures as high as 1200–1300°C. Despite there are some works dedicated to the study of the alumina behaviour when subjected to thermal shock (Saâdaoui and Fantozzi, 1998; Hahn and Lee, 1999; Lee et al., 2002; Dimitrijevic et al., 2013; Belghalem et al., 2014; Li et al., 2016) we do not know any experimental work dealing with the behaviour of alumina when subjected to high-temperatures cycles at the surface of the test-pieces with rapid cooling/heating conditions. Therefore, the primary goal of this work is to evaluate the performance of test-pieces (circular discs with 25 mm diameter and 2 mm thickness) of a commercial grade of high-purity dense monolithic Alumina (RAPAL® 100) when it is exposed to rapid cycles of temperature variation.

The creation of rapid cycles of temperature variation at the surface of a test-piece is not easy to achieve using the traditional heating-systems, whatever they are: fuel or gas combustion furnaces, electric resistance furnaces, induction furnaces, or even microwave furnaces. However, one way to generate rapid variations of temperature is by direct exposure of the test-piece to concentrated solar radiation. Some examples of the use of concentrated solar radiation for rapid heating and thermal cycling are available in the literature (Douale et al., 1999; Kováčik et al., 2014; Sallaberry et al., 2015).

2 MATERIAL AND TESTS

2.1 RAPAL® 100 Alumina Discs

The alumina produced by Rauschert company with a purity grade of 99.7% bears the trade names of RAPAL® 200 or RAPAL® 100. This type of alumina possesses a density close to the theoretical value, because is practically free of porosity. It presents excellent properties, namely: very high hardness which gives the pieces a high wear resistance; high mechanical strength; good temperature resistance up to 1650°C; good/moderate thermal conductivity; it is an electrical isolator even at high temperatures; it is corrosion resistant in diluted acids and lyes; it allows highly polished surfaces, which show low-friction coefficient.

As mentioned in the Introduction, in the present work we have used circular discs, with 25 mm diameter and 2 mm thickness, made of commercial high-purity dense monolithic alumina RAPAL® 100.

According to the manufacturer (the Rauschert company), the discs were produced through uniaxial pressing. The starting powder mean particle size (d_{50}) is 1 micron, with a specific area of 2.11 m²/g (BET). The powder compacting pressure is 100 MPa, applied at ambient temperature. After being compacted, the discs are sintered at 1635°C with a holding time of 150 minutes. The following properties of RAPAL® 100 are mentioned by the manufacturer (Rauschert data sheet, 2018): density: > 3.85 g/cm³; uniaxial flexural strength: 300 MPa; Young's modulus: 380 GPa; Mohs hardness: 9; Vickers hardness HV_{0.1}: 1700–2300; linear thermal expansion coefficient (in the range 20–1000°C): 9×10^{-6} K⁻¹; thermal conductivity: 19–30 W m⁻¹ K⁻¹; electrical resistivity at 20°C: 10¹⁴ Ω.cm.

2.2 High Temperature Cycles

Tests with rapid heating-cooling cycles were carried out thanks to the capabilities and characteristics of a high-power solar furnace: the 60 kW power solar furnace SF60 of the Plataforma Solar de Almería, in Spain. A schematic of the solar furnace test system for obtaining a concentrated solar beam horizontally oriented towards the target is shown in Figure 1. In the case of SF60, the solar direct radiation is reflected by a 130 m² flat heliostat (placed outside the building) onto a fixed parabolic concentrator (inside the building) composed of 89 facets (curved mirrors) which altogether make a total of 100 m² parabolic-shape reflecting surface area (see Figure 2). The parabolic concentrator reflects and concentrates the sunlight on a focal area where the test setup is installed. The solar flux can be controlled by adjusting the opening of the shutter or attenuator; and hence it is the opening percentage of the shutter that controls the temperature in the test setup. In our experiments, a 45° inclined mirror was placed before the focal area so that the concentrated solar beam becomes vertically oriented towards the target. The 45° inclined mirror is depicted in Figure 2.

The test setup placed at the focal area is depicted in Figures 3 and 4 in order to explain the positioning of the discs and the location of the thermocouples that were used to measure the temperature at various locations in the vicinity of the alumina discs. Figure 3 shows six discs of RAPAL® 100 duly positioned on a zirconia felt and ready to be irradiated by concentrated sunlight. During this work, 36 identical discs were exposed to the thermal cycles, in groups of 6 + 6 = 12 discs.

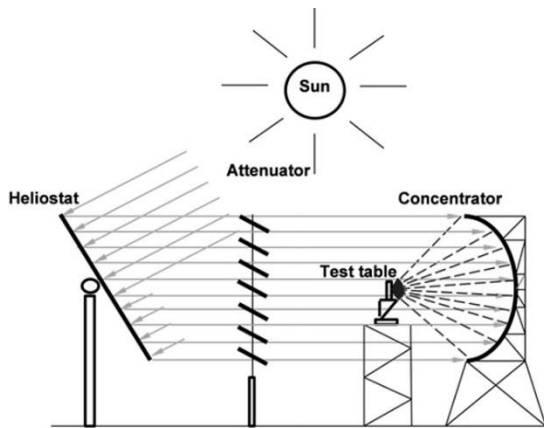


Figure 1: Schematics of SF60 test system at Plataforma Solar de Almería (Martínez Plaza, 2013).



Figure 2: Parabolic concentrator, 45° inclined mirror and the test table of SF60 solar furnace.

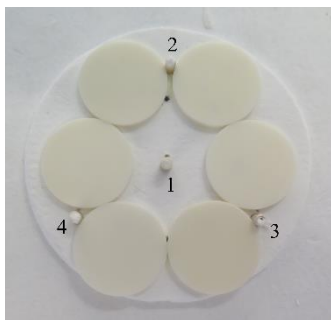


Figure 3: Discs of RAPAL® 100 ready to be irradiated.

For measuring the temperature at various locations in the vicinity of the discs, twelve type K thermocouples were used. Figure 4 shows the locations of the thermocouples' joints, after removing the discs, the zirconia felt, and the alumina thermocouple protection sheaths.

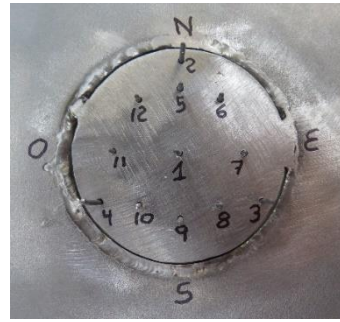


Figure 4: Locations of the thermocouples' joints.

For obtaining a more homogeneous distribution of temperature at the surface of the discs, a device (named "homogenizer") composed of vertical mirrors was placed close to the focal zone. The distribution of temperature was also evaluated using an infra-red camera and its software (see Figure 5); characteristics of IR CAM model: Equus 327k SM PRO; detector: Indium Antimonide (InSb) focal plane array (FPA); resolution: 327 680 (640 × 512) pixels; spectral range: 1.5 μm to 5 μm (SM).

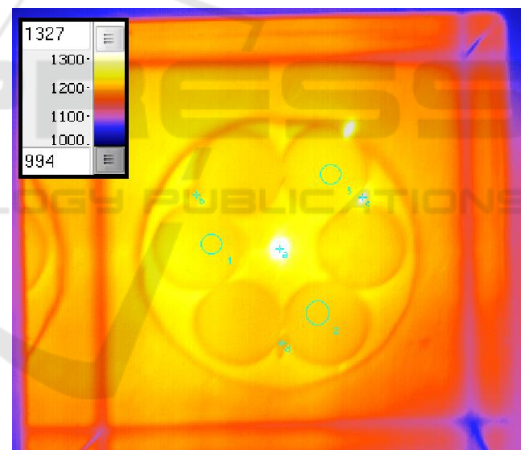


Figure 5: Image obtained by the IR CAM software.

To generate rapid heating-cooling cycles at the surface of the irradiated discs, an automatic system was developed composed by a plate with reciprocating motion, i.e. with a repetitive back-and-forth linear motion. This type of horizontal shutter is placed close to the focal zone in order to interfere with solar radiation flux before it irradiates the discs. The cooling of the discs can be accelerated by blowing them with compressed air.

Table 1: Groups of discs and corresponding heating-cooling cycles.

	No. of thermal cycles	Temperature at central thermocouple		Total duration of 100 cycles
		Maximum	Minimum	
Group A	100	1200°C	900°C	≈ 35 minutes
Group B	100	1200°C	400°C	≈ 150 minutes
Group C	100	1200°C	400°C	≈ 77 minutes

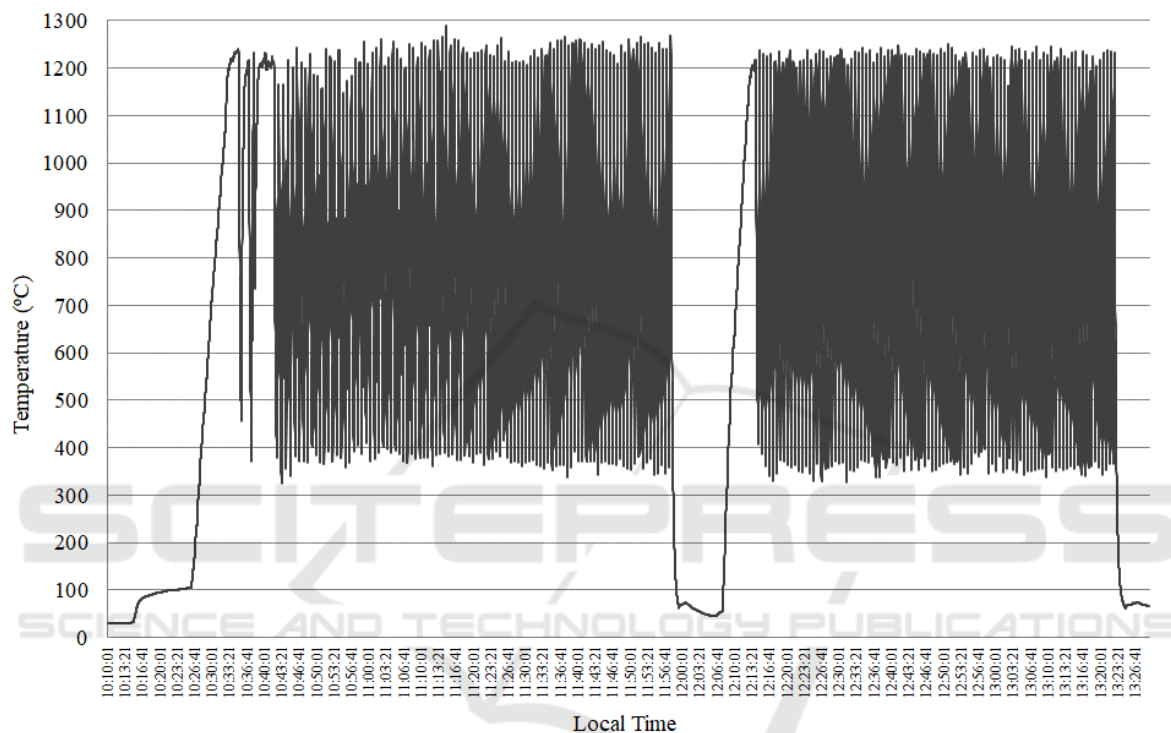


Figure 6: Example of heating-cooling cycles.

All discs were exposed to 100 heating-cooling cycles with the same maximum temperature, $T_{\max} = 1200^{\circ}\text{C}$, measured by the thermocouple with the reference number 1 (located at the centre). Table 1 summarizes the differences among the heat treatments applied to the three groups of discs.

Beside these three groups (each one composed of 12 discs) that were exposed to the thermal cycling, another group of 12 unexposed discs was used for assessing the mechanical properties before the thermal cycling.

An example of the heating-cooling cycles obtained by exposure of the discs to concentrated solar radiation is shown in Figure 6: the thermal cycling of group C discs ($T_{\max} \approx 1200^{\circ}\text{C}$; $T_{\min} \approx 400^{\circ}\text{C}$). In this case, 6 discs were exposed to 100 cycles between 10:36 and 11:56 (local time) and then

other 6 discs were exposed to 100 cycles between 12:13 and 13:23 (local time). In solar furnaces it is a tradition to register the temperatures versus the local time (hour of the day). We need the best insolation conditions to attain high-temperature in the experiments. In our experiments the solar radiation reaching the heliostat was in range of $700 - 840 \text{ W/m}^2$ depending on the hour and weather conditions during the day.

A close view of variation of temperature versus time for two thermal cycles (in the period between 12:39:40 and 12:41:10 of Figure 6) is shown in Figure 7. The temperature indicated in both Figures 6 and 7 is the temperature measured by the thermocouple located at the centre (i.e. the thermocouple with reference no. 1 in Figure 4). Heating and cooling rates must be determined from the experimental data. In the

case of Figure 7, each period of heating from 400°C till 1200°C takes circa 17 seconds; and the cooling period from 1200°C back to 400°C takes around 24 seconds.

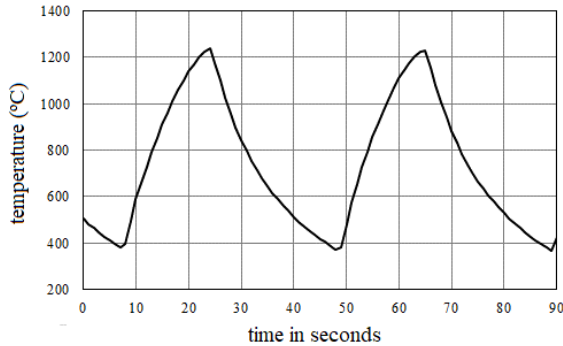


Figure 7: Temperature versus time for cycles in the period between 12:39:40 and 12:41:10 of Figure 6.

2.3 Determination of E and G

Young's modulus (E) and Coulomb's modulus (G) were determined by excitation of vibration in the discs and measurements of resonant frequencies, according to ASTM E 1876 standard test method. The equipment used was made by IMCE n.v. – Integrated Material Control Engineering (Diepenbeek, Belgium). The procedure consists in tapping the sample (disc) with a small hammer and recording the induced vibration signal with a microphone. Afterwards, the acquired vibration signal in the time domain is converted to the frequency domain by a fast Fourier transformation. Dedicated software determines the resonant frequency for each type of vibration: flexural or torsional, and then, using the classical theory of elasticity, calculates E and G values once the mass and the geometry of the test-piece are known.

2.4 Equibiaxial Flexural Strength

Figure 8 provides a schematics showing the ring-on-ring test set-up used for determination of monotonic equibiaxial flexural strength at ambient temperature, according to ASTM C 1499 standard test method. A self-aligning ring-on-ring jig that generates the equibiaxial flexure is placed between compression plates in a universal mechanical testing machine (Instron 5566 equipped with a 10 kN load cell). The test-piece (alumina disc) is compressed between two concentric rings with different diameter. In our experiments, the crosshead velocity of the testing machine was 0.5 mm per minute. Figure 9 depicts a

group of alumina discs after being fractured by the ring-on-ring test procedure.

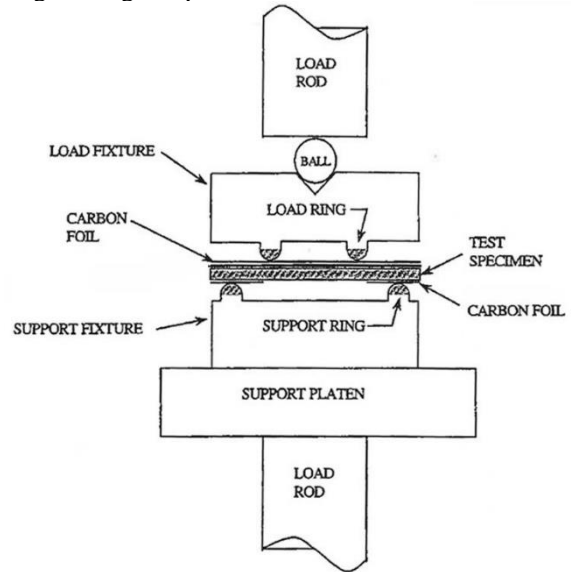


Figure 8: Section view of basic fixturing and test specimen for equibiaxial testing according to ASTM C 1499.



Figure 9: A group of alumina discs after ring-on-ring tests.

The flexural strength σ_R in equibiaxial conditions is given by (Fernandes and Rosa, 1991):

$$\sigma_R = \frac{3F}{2\pi h^2} \times \left[(1-\nu) \frac{D_S^2 - D_i^2}{2D^2} + (1+\nu) \ln \frac{D_S}{D_i} \right] \quad (3)$$

where F refers to the rupture load, h the specimen thickness, ν the Poisson's ratio of the specimen material, D_S the diameter of the lower ring (20.2mm), D_i the diameter of the upper ring (10.1 mm), and D the diameter of the test-piece (alumina disc).

Table 2. Average values (\pm standard deviation) of properties before and after heating-cooling cycles.

	Density [g/cm ³]	E [GPa]	G [GPa]	Flexural Strength [MPa]
Before: reference group	3.91 \pm 0.01	364 \pm 7	158 \pm 2	244 \pm 46
After: Group A	3.93 \pm 0.01	369 \pm 8	159 \pm 2	238 \pm 37
After: Group B	3.92 \pm 0.01	363 \pm 7	157 \pm 2	211 \pm 34
After: Group C	3.92 \pm 0.01	362 \pm 6	158 \pm 2	242 \pm 31

3 RESULTS AND DISCUSSION

The results obtained from the experiments allow to compare the values of the properties before and after exposure to thermal cycling. This was the rationale used to evaluate the possible degradation of the alumina when exposed to rapid thermal cycles at high-temperature. Table 2 summarizes the average (\pm standard deviation) values obtained for the following properties of RAPAL[®] 100: density (determined by Archimedes method); Young's modulus of elasticity (E); Coulomb's modulus of elasticity (G); and equibiaxial flexural strength.

In the whole literature, we did not find other researchers' results for comparison, because the thermal cycling experiments described in this work are very difficult to be performed with conventional furnaces; and therefore the results obtained in the present work are relevant. They have demonstrated the good quality of RAPAL[®] 100 and its adequacy for high temperature applications. We have not observed any rupture in the alumina discs during their exposure to the thermal cycles. None of the different sequences of 100 cycles (even the most severe one with 100 cycles applied in 77 minutes, with maximum temperature of 1200°C and minimum temperature of 400°C) has caused noticeable alterations in the studied properties (density; Young's modulus of elasticity; Coulomb's modulus of elasticity; flexural strength) when comparing the values before and after applying the heating-cooling cycles. The only perceptible difference it is practically negligible; it consists in the decay of flexural strength after exposure to 100 cycles in 150 minutes, with $T_{\max} = 1200^{\circ}\text{C}$ e $T_{\min} = 400^{\circ}\text{C}$; initial value is 244 (± 46) MPa and after those 100 cycles is 211 (± 34) MPa.

According to the work of (Hahn and Lee, 1999) the critical thermal stress which makes the cracks grow catastrophically was found to be generated by the critical cooling rate, and the critical cooling rate of polycrystalline alumina ceramics was found to be a certain value: 550°C/second (Hahn and Lee, 1999). In our experiments the highest cooling rate was

approximately 34°C/s which is circa 16 times less than 550°C/s. This explains why we did not notice any crack propagation in the test-pieces, even after 100 cycles; as well as we did not obtain any relevant statistical changes in the mechanical properties.

The value of Young's modulus mentioned in the Rauschert data sheet (see section 2.1) is 380 GPa, slightly higher than the value obtained in our work, 364 (± 7) GPa, for the reference group of "as received" samples i.e. before exposure to thermal cycling (see Table 2). This small discrepancy can be explained by differences in the testing methods. Also, Rauschert data sheet mentions that uniaxial flexural strength of RAPAL[®] 100 is 300 MPa, without referring the data scatter. In our work we measured the flexural strength under equibiaxial conditions and obtained a lower average value, 244 (± 46) MPa, for the reference group i.e. before the heating-cooling cycles. These values are perfectly acceptable because the uniaxial flexural strength is typically determined under a 3-point bend test (where the sampled volume is smaller), so the probability of finding a larger critical flaw is higher in equibiaxial conditions, resulting in a lower flexural strength.

4 CONCLUSIONS

This work demonstrates that rapid variations of temperature at the surface of a material can be attained by direct exposure to highly concentrated solar radiation. For the first time, the thermal cycling behaviour of dense monolithic alumina (RAPAL[®] 100) was studied, using rapid heating-cooling cycles with a maximum temperature of 1200°C. The results prove the adequacy of this material for high temperature applications subjected to rapidly changing thermal conditions.

ACKNOWLEDGEMENTS

This research has been partially funded by the European Commission in the frame of the SFERA-II project (FP7, Grant. Agreement 312643) and project INSHIP (Integrating National Research Agendas on Solar Heat for Industrial Processes) www.inship.eu.

REFERENCES

- Belghalem, H., Hamidouche, M., Gremillard, L., Bonnefont, G., Fantozzi, G., 2014. Thermal shock resistance of two micro-structured alumina obtained by natural sintering and SPS. *Ceram. Int.* 40, 619–627.
- Dimitrijevic, M.M., Medjo, B., Heinemann, R.J., Rakin, M., Volkov-Husovic, T., 2013. Experimental and numerical analysis of thermal shock damages to alumina based ceramic disk samples. *Mater. Des.* 50, 1011–1018.
- Douale, P., Serror, S., Duval, R.M.P., Serra, J.J., Felder, E., 1999. Thermal shocks on an electrolytic chromium coating in a solar furnace. *Journal de Physique IV* 9, 429–434.
- Evans, A.G., Linzer, M., Johnson, H., Hasselman, D.P.H., Kipp, M.E., 1975. Thermal fracture studies in ceramic systems using an acoustic emission technique. *J. Mater. Sci.* 10, 1608–1615.
- Fernandes, J.J., Rosa, L.G., 1991. Ensaaios biaxiais de cerâmicos. *Actas V Encontro Nacional da Sociedade Portuguesa de Materiais*, Lisboa, Vol.1, pp 375–384, doi: 10.13140/RG.2.1.2589.6809.
- Hahn, B.S., Lee, H.L., 1999. Effect of environmental factors on thermal shock behaviour of polycrystalline alumina ceramics. *J. Mater. Sci.* 34, 3623–3630.
- Hirata, Y., 2015. Theoretical analyses of thermal shock and thermal expansion coefficients of metals and ceramics. *Ceram. Int.* 41, 1145–1153.
- Kováčik, J., Emmer, S., Rodriguez, J., Cañadas I., 2014. Solar furnace: thermal shock behaviour of TiB₂ coating on steel. *Proceedings of METAL 2014*, pp 863–868. Tanger Ltd, Ostrava, Czech Republic.
- Lee, J.H., Park, S.E., Lee, H.J., Lee, H.L., 2002. Thermal shock behaviour of alumina ceramics by ball-on-3-ball test. *Mater. Lett.* 56, 1022–1029.
- Li, D.Y., Li, W.G., Wang, R.Z., Kou, H.B., 2016. Influence of thermal shock damage on the flexure strength of alumina ceramic at different temperatures. *Mater. Lett.* 173, 91–94.
- Martínez Plaza, D., 2013. Desarrollo de dispositivo para producción de energía térmica a partir de un receptor solar de tipo volumétrico y estudio de su aplicabilidad a procesos de alta temperatura para fabricación industrial de cerámicas, PhD thesis, Universidad de Sevilla.
- Rauschert data sheet, 2018. Available at: https://rauschert.com/images/documents/products/technical-ceramics/Rapal_Tabelle.pdf
- Saâdaoui, M., Fantozzi, G., 1998. Crack growth resistance under thermal shock loading of alumina. *Mater. Sci. Eng. A247*, 142–151.
- Sallaberry, F., García de Jalón, A., Zaversky, F., Vázquez, A.J., López-Delgado A., Tamayo, A., Mazo, M.A., 2015. Towards standard testing materials for high temperature solar receivers. *Energy Procedia* 69, 532–542.